

${}^4\text{He}+n+n$ continuum within an *ab initio* framework

Carolina Romero-Redondo,^{1,*} Sofia Quaglioni,^{2,†} Petr Navrátil,^{1,‡} and Guillaume Hupin^{2,§}

¹*TRIUMF, 4004 Wesbrook Mall, Vancouver, British Columbia, V6T 2A3, Canada*

²*Lawrence Livermore National Laboratory, P.O. Box 808, L-414, Livermore, California 94551, USA*

(Dated: February 28, 2022)

The low-lying continuum spectrum of the ${}^6\text{He}$ nucleus is investigated for the first time within an *ab initio* framework that encompasses the ${}^4\text{He}+n+n$ three-cluster dynamics characterizing its lowest decay channel. This is achieved through an extension of the no-core-shell model combined with the resonating-group method, in which energy-independent non-local interactions among three nuclear fragments can be calculated microscopically starting from realistic nucleon-nucleon interactions and consistent *ab initio* many-body wave functions of the clusters. The three-cluster Schrödinger equation is solved with three-body scattering boundary conditions by means of the hyperspherical-harmonic method on a Lagrange mesh. Using a soft similarity-renormalization-group evolved chiral nucleon-nucleon potential, we find the known $J^\pi = 2^+$ resonance as well as a result consistent with a new low-lying second 2^+ resonance recently observed at GANIL at 2.6 MeV above the ${}^6\text{He}$ ground state. We also find resonances in the 2^- , 1^+ and 0^- channels, while no low-lying resonances are present in the 0^+ and 1^- channels.

PACS numbers: 21.60.De, 25.10.+s, 27.20.+n

Introduction. Nuclear systems near the drip lines, the limits of the nuclear chart beyond which neutrons or protons start dripping out of nuclei, offer an exciting opportunity to advance our current understanding of the interactions among nucleons, so far mostly based on the study of stable nuclei. This is not a goal devoid of challenges. Experimentally, the study of these rare nuclei with atypical neutron-to-proton ratios is challenged by their short half lives and minute production cross sections. A major stumbling block in nuclear theory has to deal with the low breakup thresholds, which cause bound, resonant and scattering states to be strongly coupled. Particularly arduous in this respect are those systems for which the lowest threshold for particle decay is of the three-body nature, such as ${}^6\text{He}$, which decays into an α particle (${}^4\text{He}$ nucleus) and two neutrons at the excitation energy of 0.975 MeV. Aside from a narrow resonance characterized by spin-parity $J^\pi = 2^+$, located at 1.8 MeV above the ground state (g.s.), the positions, spins and parities of the excited states of this nucleus are still under discussion. Experimentally the picture is not clear. Proton-neutron exchange reactions between two fast colliding nuclei produced resonant-like structures around 4 [1] and 5.6 [2] MeV of widths $\Gamma \sim 4$ and 10.9 MeV, respectively, as well as a broad asymmetric bump at ~ 5 MeV [3], but disagree on the nature of the underlying ${}^6\text{He}$ excited state(s). While the structures of Refs. [1] and [3] are explained as dipole excitations compatible with oscillations of the positively-charged ${}^4\text{He}$ core against the halo neutrons, that of Ref. [2] is identified as a second 2^+ state. More recently, a much narrower 2^+ ($\Gamma = 1.6$ MeV) state and a $J = 1$ resonance ($\Gamma \sim 2$ MeV) of unassigned parity were populated at 2.6 and 5.3 MeV, respectively, with the two-neutron transfer reaction ${}^8\text{He}(p, {}^3\text{H}){}^6\text{He}^*$ [4]. On the theory side, several predictions all incomplete in dif-

ferent ways suggest a $2_1^+, 2_2^+, 1^+, 0^+$ sequence of levels above the first excited state but disagree on the positions and widths. Those from six-body calculations with realistic Hamiltonians [5–7] were obtained within a bound-state approximation and cannot provide any information about the widths of the levels. *Vice versa*, those from three-body models [8, 9], from microscopic three-cluster models [10, 11] or from calculations hinging on a shell-model picture with inert ${}^4\text{He}$ core [12, 13] can describe the continuum, but were obtained using schematic interactions and a simplified description of the structure. In this Letter we present the first *ab initio* calculation of the ${}^4\text{He}+n+n$ continuum starting from a nucleon-nucleon (NN) interaction that describes two-nucleon properties with high accuracy.

Formalism. In the no-core shell model combined with the resonating-group method (NCSM/RGM), A -body bound and/or scattering states characterized by three-cluster configurations are described by the wave function

$$|\Psi^{J^\pi T}\rangle = \sum_\nu \iint dx dy x^2 y^2 \hat{A}_\nu |\Phi_{\nu xy}^{J^\pi T}\rangle [\mathcal{N}^{-\frac{1}{2}} \chi]_\nu^{J^\pi T}(x, y), \quad (1)$$

in terms of $(A - a_{23}, a_2, a_3)$ ternary cluster channels

$$\begin{aligned} |\Phi_{\nu xy}^{J^\pi T}\rangle &= \left[(|A - a_{23} \alpha_1 I_1^{\pi_1} T_1\rangle |a_2 \alpha_2 I_2^{\pi_2} T_2\rangle |a_3 \alpha_3 I_3^{\pi_3} T_3\rangle)^{(s_{23} T_{23})} \right]^{(ST)} \\ &\times (Y_{\ell_x}(\hat{\eta}_{23}) Y_{\ell_y}(\hat{\eta}_{1,23}))^{(L)} \left]^{(J^\pi T)} \frac{\delta(x - \eta_{23})}{x \eta_{23}} \frac{\delta(y - \eta_{1,23})}{y \eta_{1,23}} \end{aligned} \quad (2)$$

built within a translation-invariant harmonic oscillator (HO) basis from NCSM eigenstates of each of the three clusters, $|A - a_{23} \alpha_1 I_1^{\pi_1} T_1\rangle$, $|a_2 \alpha_2 I_2^{\pi_2} T_2\rangle$ and $|a_3 \alpha_3 I_3^{\pi_3} T_3\rangle$, and antisymmetrized with an appropriate operator \hat{A}_ν to preserve the Pauli exclusion principle exactly. Here

$A - a_{23}, a_2$, and a_3 (with $A \geq a_{23} = a_2 + a_3$) indicate the mass numbers of the three clusters having angular momentum, parity, isospin and energy quantum numbers $I_i^{\pi_i} T_i$ and α_i ($i = 1, 2, 3$). Each channel is identified by its total isospin, angular momentum and parity ($J^{\pi} T$) and an index ν specifying all other quantum numbers, i.e., $\nu = \{A - a_{23} \alpha_1 I_1^{\pi_1} T_1; a_2 \alpha_2 I_2^{\pi_2} T_2; a_3 \alpha_3 I_3^{\pi_3} T_3; s_{23} T_{23} S \ell_x \ell_y L\}$. Further, $\tilde{\eta}_{1,23} = \eta_{1,23} \hat{\eta}_{1,23}$ and $\tilde{\eta}_{23} = \eta_{23} \hat{\eta}_{23}$ are relative coordinates proportional, respectively, to the displacement between the center of mass (c.m.) of the first cluster and that of the residual two fragments, and to the distance between the c.m.'s of clusters 2 and 3.

Introducing the hyperspherical coordinates $\rho = \sqrt{x^2 + y^2}$ and $\alpha = \arctan \frac{x}{y}$, the relative motion wave functions among the clusters,

$$\chi_{\nu}^{J^{\pi} T}(\rho, \alpha) = \frac{1}{\rho^{5/2}} \sum_K u_{\nu K}^{J^{\pi} T}(\rho) \phi_K^{\ell_x, \ell_y}(\alpha), \quad (3)$$

can be expanded over the complete set $\phi_K^{\ell_x, \ell_y}(\alpha)$, the hyperangular part of the hyperspherical harmonics $\mathcal{Y}_{LM_L}^{K \ell_x \ell_y}(\Omega) = \phi_K^{\ell_x, \ell_y}(\alpha) (Y_{\ell_x}(\hat{\eta}_{23}) Y_{\ell_y}(\hat{\eta}_{1,23}))_{M_L}^{(L)}$. The unknown amplitudes $u_{\nu K}^{J^{\pi} T}(\rho)$ are then found by solving the nonlocal hyperradial equations

$$\sum_{K'} \int d\rho \rho^5 \bar{\mathcal{H}}_{\nu\nu'}^{K'K}(\rho', \rho) \frac{u_{K\nu}^{J^{\pi} T}(\rho)}{\rho^{5/2}} = E \frac{u_{K'\nu'}^{J^{\pi} T}(\rho')}{\rho'^{5/2}}, \quad (4)$$

where $\bar{\mathcal{H}}_{\nu\nu'}^{K'K}(\rho', \rho) = [\mathcal{N}^{-\frac{1}{2}} \mathcal{H} \mathcal{N}^{-\frac{1}{2}}]_{\nu\nu'}^{K'K}(\rho', \rho)$ is the orthogonalized kernel obtained from the Hamiltonian and overlap (or norm) matrix elements

$$\mathcal{H}_{\nu\nu'}^{J^{\pi} T}(x', y', x, y) = \langle \Phi_{\nu'x'y'}^{J^{\pi} T} | \hat{\mathcal{A}}_{\nu'} H \hat{\mathcal{A}}_{\nu} | \Phi_{\nu xy}^{J^{\pi} T} \rangle, \quad (5)$$

$$\mathcal{N}_{\nu\nu'}^{J^{\pi} T}(x', y', x, y) = \langle \Phi_{\nu'x'y'}^{J^{\pi} T} | \hat{\mathcal{A}}_{\nu'} \hat{\mathcal{A}}_{\nu} | \Phi_{\nu xy}^{J^{\pi} T} \rangle, \quad (6)$$

after projection over the basis $\phi_K^{\ell_x, \ell_y}(\alpha)$. Equation (4) is solved with either bound- or genuinely three-body scattering-state (i.e. no bound two-body subsystems are present) boundary conditions by means of the microscopic R -matrix method on a Lagrange mesh [14–18]. For more details on the three-cluster NCSM/RGM formalism we refer the interested reader to Ref. [19], where we first applied the approach to the description of the ground state of ${}^6\text{He}$ within a ${}^4\text{He}+n+n$ basis ($a_2, a_3 = 1$). Here we apply the same framework to the much more challenging problem of the continuum of this system.

Results. The present calculations are based on the chiral $\text{N}^3\text{LO NN}$ [20] interaction softened via the Similarity Renormalization Group (SRG) to minimize the influence of momenta higher than $\Lambda = 1.5 \text{ fm}^{-1}$. This soft potential permits us to reach convergence in the HO expansions within $N_{\text{max}} \sim 13$ quanta, the largest model space presently achievable. At the same time, it also

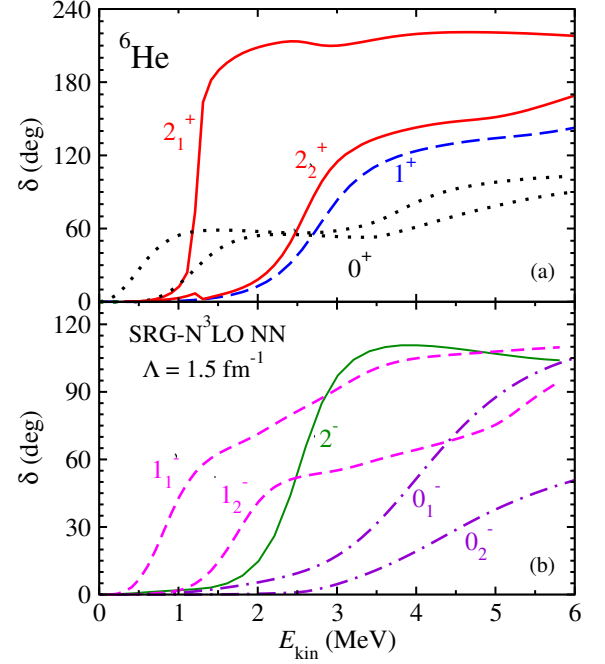


FIG. 1. (Color online) Calculated ${}^4\text{He}+n+n$ (a) positive- and (b) negative-parity attractive eigenphase shifts (except for the 2^+ and 1^+ channels, where the diagonal phase shifts are shown) as a function of the three-cluster kinetic energy in the c.m. frame E_{kin} . See the text for further details.

leads to a ${}^4\text{He}$ g.s. energy [21, 22] and $n+{}^4\text{He}$ phase shifts [23] close to experiment despite the omission of three-nucleon ($3N$) forces, which are beyond the scope of this first *ab initio* study of the ${}^4\text{He}+n+n$ continuum.

We further describe the ${}^4\text{He}$ cluster only by its $I_1^{\pi_1} T_1 =$

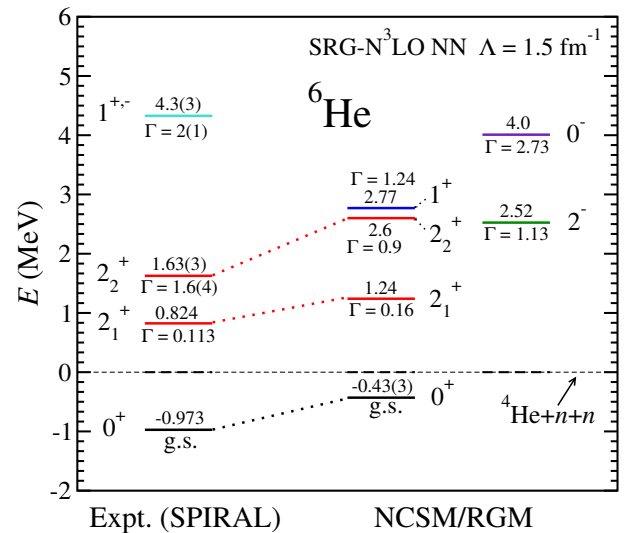


FIG. 2. (Color online). Comparison of the spectrum obtained within this work using the NCSM/RGM to the experimental spectrum measured at the SPIRAL facility (GANIL) [4].

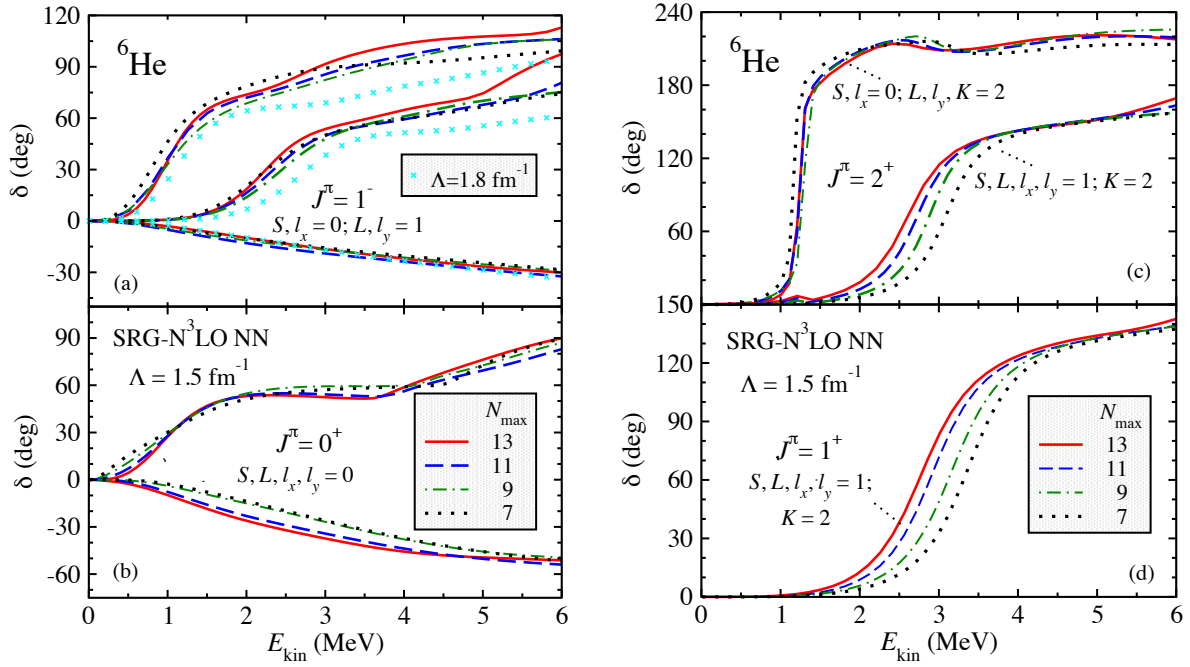


FIG. 3. (Color online) Convergence behavior of calculated ${}^4\text{He}+n+n$ (a) $J^\pi = 1^-$ and (b) 0^+ eigenphase shifts at $K_{\text{max}} = 19$ and 28, respectively, and (c) 2^+ and (d) 1^+ diagonal phase shifts at $K_{\text{max}} = 20$ with respect to the size N_{max} of the NCSM/RGM model space. For these calculations we used an extended HO model space of $N_{\text{ext}} = 70$ and a matching radius of $a = 30 \text{ fm}$. In panel (a), $N_{\text{max}} = 11$ 1^- phase shifts obtained with the $\Lambda = 1.8 \text{ fm}^{-1}$ SRG NN potential are shown for comparison.

0^+0 g.s. and ignore core polarization effects, which have been estimated to account for $\sim 5\%$ of the ${}^6\text{He}$ binding energy [19]. The inclusion of excited states of the core leads to a (presently) unbearable increment of the computational size of the problem. This will be overcome in the future by coupling the present three-cluster model space with eigenstates of the six-body system within the no-core shell model with continuum (NCSMC) [24, 25].

We solve Eq. (4) for the $J^\pi = 0^\pm, 1^\pm, 2^\pm$ channels, and extract the corresponding phase shifts from the diagonal elements of the three-body scattering matrix or from its diagonalization, when large off-diagonal couplings are present. A summary of the obtained low-lying attractive phase shifts is presented in Fig. 1. We have identified several resonances. The lowest and sharpest appears in the 2^+ channel around 1.25 MeV above the ${}^4\text{He}+n+n$ threshold. An analysis of this resonance, corresponding to the very well known first excited state of ${}^6\text{He}$, shows that it is dominated by 1S_0 neutrons in an $\ell_y = 2$ relative motion with respect to the ${}^4\text{He}$ g.s. ($S, l_x = 0; L, l_y, K = 2$). A second broader 2^+ resonance emerges at $\sim 2.6 \text{ MeV}$, where the prevalent picture is that of the halo neutrons with aligned spins, moving relative to each other and to the core in P wave ($S, l_x, L, l_y = 1; K = 2$). The same structure also characterizes a 1^+ resonance located at slightly higher energy. Resonances also appear in the 2^- and 0^- channels, dominated by $S, l_x, L = 1$ and $\ell_y = 0$ quantum numbers. On the other hand, the homogeneous growth through 90° characteristic of a resonance is not

present in the 1^- or in the 0^+ channels. Therefore we cannot see any evidence of a low-lying state that could be identified with the 1^- soft dipole mode suggested in Refs. [1] and [3]. In addition, our results do not support the presence of a low-lying 0^+ monopole resonance above the 1^+ state reported by previous theoretical investigations of the ${}^4\text{He}+n+n$ continuum, in which the ${}^4\text{He}$ was considered as an inert particle with no structure. These three-body calculations, performed within the hyperspherical harmonics basis [8, 9, 26, 27] and with the complex scaling method [28, 29], obtained a similar sequence of $2_1^+, 2_2^+, 1^+$ and 0_2^+ levels, but different resonance positions and widths. (Only the first two 2^+ resonances were shown in Ref. [27].) Microscopic ${}^4\text{He}+n+n$ calculations based on schematic interactions were later reported in Refs. [10, 11], but showed only results for the 2_1^+ narrow resonance and do not comment on a 0^+ excited state.

In Fig. 2, the energy spectrum of states extracted from the resonances of Fig. 1 is compared to the one recently measured at GANIL [4]. Our results are consistent with the presence of the second low-lying narrow 2^+ resonance observed for the first time in this experiment. A $J = 1$ resonance was also measured at 4.3 MeV, however, the parity of such state is not yet determined and is not possible to univocally identify it with the 1^+ resonance found at 2.77 MeV in the present calculations. At the same time, the energy-dependence of the 1^- eigenphase shifts of Fig. 1(b) does not favor the interpretation of this low-

lying state as a dipole mode. We also predict two broader negative-parity states not observed.

A thorough study of the convergence of the results with respect to all parameters defining the size of our model space was performed. These are the maximum value K_{\max} of the hyperangular momentum in the expansion (3); the size N_{\max} of the HO basis used to calculate the g.s. of ${}^4\text{He}$ and the localized parts of Eqs. (5) and (6); and finally, the size $N_{\text{ext}} \gg N_{\max}$ of the extended HO basis used to represent a delta function in the core-halo distance entering the portion of the Hamiltonian kernel that accounts for the interaction between the halo neutrons (see Eq. (39) of Ref. [19]). In each case the number of integration points and the hyperradius a used to match internal and asymptotic solutions within the R -matrix method on Lagrange mesh were chosen large enough to reach stable, a -independent results. All calculations were performed with the same $\hbar\Omega = 14$ MeV frequency adopted for the study of the ${}^6\text{He}$ g.s. [19].

We first set the extended HO basis size to the value ($N_{\text{ext}} = 70$) we found to be sufficient for the 0^+ g.s. energy [19], and established that expansion (3) converges at $K_{\max} = 19/20$ for all negative/positive-parity channels except the 0^+ , requiring $K_{\max} = 28$. Examples of the convergence pattern with respect to the HO basis size N_{\max} are shown in Fig. 3. In general convergence is satisfactory at $N_{\max}=13$. For the higher-lying resonances this value is not quite sufficient, but already provides the qualitative behavior to start discussing the continuum structure of the system. Next we study the dependence on N_{ext} , which regulates the range of the potential kernel. Not unexpectedly, an increase of N_{ext} requires at the same time incrementing the matching hyperradius a needed to reach the asymptotic region (we used values of up to 60 fm) and K_{\max} , for which we used values as high as 40 in the 0^+ channel. This limited the maximum value of N_{ext} used to obtain our best ($N_{\max} = 13$) results for the 0^+ , 1^- , and 2^+ results of Figs. 1 and 2 to 200, 110, and 90, respectively. As shown in Fig. 4, the influence of N_{ext} is most pronounced for attractive phase shifts in which the two neutrons are in 1S_0 relative motion. There the nn interaction is larger and the wave function is more extended due to the Pauli exclusion principle. By far the dominating effect is the steeper onset of the 0^+ attractive eigenphase shifts that, as already noted in Ref. [27], becomes more accentuated for (higher-lying) components with $K > 0$. However, the qualitative results remain unchanged. In particular, the value of N_{ext} has little or no influence on the position and width of the resonances. Also, the binding energy of the 0^+ ground state of ${}^6\text{He}$ calculated in [19] remains unchanged within this much larger model space. Finally, changing the value of the SRG parameter used to soften the NN interaction to $\Lambda = 1.8 \text{ fm}^{-1}$ does not change the overall structure of the continuum states. Bearing in mind that with this harder potential convergence is slower, in each channel

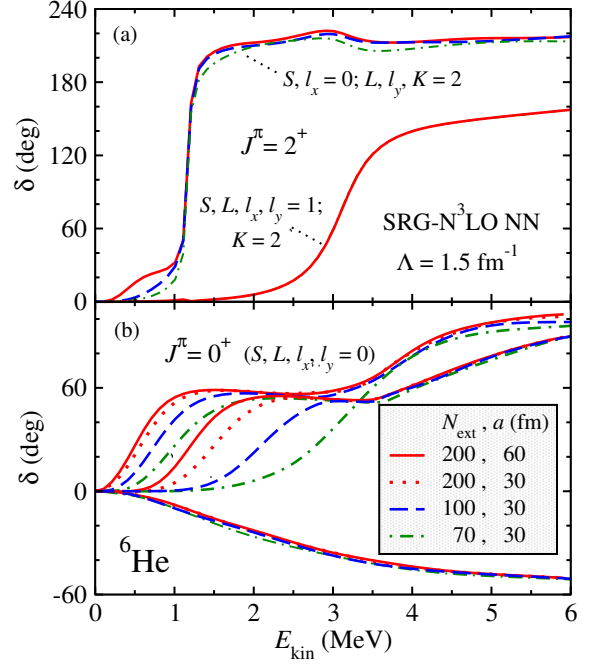


FIG. 4. (Color online) Dependence on the size of the extended HO model space N_{ext} of calculated ${}^4\text{He}+n+n$ (a) $J^\pi = 2^+$ diagonal phase shifts at $N_{\max} = 7$, and (b) 0^+ eigenphase shifts at $N_{\max} = 13$. The curves overlap for the 2_2^+ resonance.

we obtain the same number of resonances with similar widths, though somewhat shifted in energy (less than 1 MeV), as shown in Fig. 3 for the 1^- . This is evidence that the softness of the potential used is not introducing any spurious resonances and, therefore, verifies the reliability of our results.

Conclusions. We calculated, for the first time within an *ab initio* approach, the continuum spectrum of ${}^6\text{He}$ as a ${}^4\text{He}+n+n$ system. Given the low two-neutron separation energy of this nucleus, including the three-cluster basis in the calculation is essential. We found several resonances, including the well-known narrow 2_1^+ and the recently measured broader 2_2^+ . Additional resonant states emerged in the 2^- , and 1^+ channels near the second 2^+ resonance, and in the 0^- at slightly higher energy. We found no evidence of low-lying resonances in the 0^+ and 1^- channels. Therefore, our results do not support the idea that the accumulation of dipole strength at low energy is originated by a three-body 1^- resonance.

The inclusion of $3N$ forces and core polarization effects through the NCSMC coupling are underway and will increase the predictive capability of the method. Finally, we expect that complementing this approach with the use of two integral relations derived from the Kohn variational principle [30–32] will increase the range of systems that can be described by limiting the distance for which the wave function has to be calculated. This will be essential for the study of ${}^{11}\text{Li}$ within a ${}^9\text{Li}+n+n$ basis.

Computing support for this work came from the LLNL institutional Computing Grand Challenge program and from an INCITE Award on the Titan supercomputer of the Oak Ridge Leadership Computing Facility (OLCF) at ORNL. We thank the Institute for Nuclear Theory at the University of Washington for its hospitality and the Department of Energy for partial support during the completion of this work. Prepared in part by LLNL under Contract DE-AC52-07NA27344. Support from the NSERC Grant No. 401945-2011 and U.S. DOE/SC/NP (Work Proposal No. SCW1158) is acknowledged. TRIUMF receives funding via a contribution through the Canadian National Research Council.

* cromeroredondo@triumf.ca

† quaglioni1@llnl.gov

‡ navratil@triumf.ca

§ hupin1@llnl.gov

- [1] S. Nakayama, T. Yamagata, H. Akimune, I. Daito, H. Fujimura, Y. Fujita, M. Fujiwara, K. Fushimi, T. Inomata, H. Kohri, N. Koori, K. Takahisa, A. Tamii, M. Tanaka, and H. Toyokawa, *Phys. Rev. Lett.* **85**, 262 (2000).
- [2] J. Jänecke, T. Annakkage, G. P. A. Berg, B. A. Brown, J. A. Brown, G. Crawley, S. Danczyk, M. Fujiwara, D. J. Mercer, K. Pham, D. A. Roberts, J. Stasko, J. S. Winfield, and G. H. Yoo, *Phys. Rev. C* **54**, 1070 (1996).
- [3] T. Nakamura, T. Aumann, D. Bazin, Y. Blumenfeld, B. A. Brown, J. Caggiano, R. Clement, T. Glasmacher, P. A. Lofy, A. Navin, B. V. Pritychenko, B. M. Sherrill, and J. Yurkon, *Phys. Lett. B* **493**, 209 (2000).
- [4] X. Mougeot, V. Lapoux, W. Mittig, N. Alamanos, F. Auger, B. Avez, D. Beaumel, Y. Blumenfeld, R. Dayras, A. Drouart, C. Force, L. Gaudefroy, A. Gillibert, J. Guillot, H. Iwasaki, T. A. Kalanee, N. Keeley, L. Nalpas, E. C. Pollacco, T. Roger, P. Roussel-Chomaz, D. Suzuki, K. W. Kemper, T. J. Mertzimekis, A. Pakou, K. Rusek, J.-A. Scarpaci, C. Simenel, I. Strojek, and R. Wolski, *Phys. Lett. B* **718**, 441 (2012).
- [5] P. Navrátil, J. P. Vary, W. E. Ormand, and B. R. Barrett, *Phys. Rev. Lett.* **87**, 172502 (2001).
- [6] P. Navrátil and W. E. Ormand, *Phys. Rev. C* **68**, 034305 (2003).
- [7] S. C. Pieper, R. B. Wiringa, and J. Carlson, *Phys. Rev. C* **70**, 054325 (2004).
- [8] B. V. Danilin, T. Rogde, S. N. Ershov, H. Heiberg-Andersen, J. S. Vaagen, I. J. Thompson, and M. V. Zhukov, *Phys. Rev. C* **55**, R577 (1997).
- [9] B. V. Danilin, I. J. Thompson, J. S. Vaagen, and M. V. Zhukov, *Nucl. Phys. A* **632**, 383 (1998).
- [10] S. Korennoy and P. Descouvemont, *Nucl. Phys. A* **740**, 249 (2004).
- [11] A. Damman and P. Descouvemont, *Phys. Rev. C* **80**, 044310 (2009).
- [12] G. Hagen, M. Hjorth-Jensen, and J. S. Vaagen, *Phys. Rev. C* **71**, 044314 (2005).
- [13] T. Myo, K. Katō, and K. Ikeda, *Phys. Rev. C* **76**, 054309 (2007).
- [14] D. Baye, J. Goldbeter, and J.-M. Sparenberg, *Phys. Rev. A* **65**, 052710 (2002).
- [15] D. Baye, M. Hesse, J.-M. Sparenberg, and M. Vincke, *J. Phys. B: At. Mol. Opt. Phys.* **31**, 3439 (1998).
- [16] M. Hesse, J. Roland, and D. Baye, *Nucl. Phys. A* **709**, 184 (2002).
- [17] M. Hesse, J.-M. Sparenberg, F. V. Raemdonck, and D. Baye, *Nucl. Phys. A* **640**, 37 (1998).
- [18] P. Descouvemont, C. Daniel, and D. Baye, *Phys. Rev. C* **67**, 044309 (2003).
- [19] S. Quaglioni, C. Romero-Redondo, and P. Navrátil, *Phys. Rev. C* **88**, 034320 (2013).
- [20] D. R. Entem and R. Machleidt, *Phys. Rev. C* **68**, 041001 (2003).
- [21] E. D. Jurgenson, P. Navrátil, and R. J. Furnstahl, *Phys. Rev. Lett.* **103**, 082501 (2009).
- [22] E. D. Jurgenson, P. Navrátil, and R. J. Furnstahl, *Phys. Rev. C* **83**, 034301 (2011).
- [23] P. Navrátil and S. Quaglioni, *Phys. Rev. Lett.* **108**, 042503 (2012).
- [24] S. Baroni, P. Navrátil, and S. Quaglioni, *Phys. Rev. Lett.* **110**, 022505 (2013).
- [25] S. Baroni, P. Navrátil, and S. Quaglioni, *Phys. Rev. C* **87**, 034326 (2013).
- [26] S. N. Ershov, T. Rogde, B. V. Danilin, J. S. Vaagen, I. J. Thompson, and F. A. Gareev ((Russian-Nordic-British Theory (RNBT) Collaboration)), *Phys. Rev. C* **56**, 1483 (1997).
- [27] P. Descouvemont, E. M. Tursunov, and D. Baye, *Nucl. Phys. A* **765**, 370 (2006).
- [28] K. K. Shigeyoshi Aoyama, Shigeo Mukai and K. Ikeda, *Prog. Theor. Phys.* **94**, 343 (1995).
- [29] K. K. Shigeyoshi Aoyama, Shigeo Mukai and K. Ikeda, *Prog. Theor. Phys.* **93**, 99 (1995).
- [30] P. Barletta, C. Romero-Redondo, A. Kievsky, M. Viviani, and E. Garrido, *Phys. Rev. Lett.* **103**, 090402 (2009).
- [31] C. Romero-Redondo, E. Garrido, P. Barletta, A. Kievsky, and M. Viviani, *Phys. Rev. A* **83**, 022705 (2011).
- [32] A. Kievsky, M. Viviani, P. Barletta, C. Romero-Redondo, and E. Garrido, *Phys. Rev. C* **81**, 034002 (2010).